Serb. Astron. J. № 195 (2017), 23 - 31 **UDC 524.354–795**
DOI: https://doi.org/10.2298/SAJ1795023P Original scientific paper

ASCA AND XMM-NEWTON OBSERVATIONS OF THE GALACTIC SUPERNOVA REMNANT G311.5–0.3

T. G. Pannuti[1], M. D. Filipović[2], K. Luken[2], G. F. Wong[2,3], P. Manojlović[2], N. Maxted[3,2] and Q. Roper[2]

[1] *Department of Earth and Space Sciences, Morehead State University, 235 Martindale Drive, Morehead, KY 40351, USA*
E–mail: *t.pannuti@moreheadstate.edu*

[2] *Western Sydney University, Locked Bag 1797, Penrith NSW 2751, Australia*
E–mail: *m.filipovic@westernsydney.edu.au*

[3] *School of Physics, The University of New South Wales, Sydney, 2052, Australia*

(Received: July 24, 2017; Accepted: September 5, 2017)

SUMMARY: We present an analysis of X-ray observations made with *ASCA* and *XMM-Newton* of the Galactic supernova remnant (SNR) G311.5−0.3. Prior infrared and radio observations of this SNR have revealed a shell-like morphology at both wavelengths. The spectral index of the radio emission is consistent with synchrotron emission, while the infrared colors are consistent with emission from shocked molecular hydrogen. Also previous CO observations have indicated an interaction between G311.5−0.3 and an adjacent molecular cloud. Our previous analysis of the pointed *ASCA* observation made of this SNR detected X-ray emission from the source for the first time but lacked the sensitivity and the angular resolution to rigorously investigate its X-ray properties. We have analyzed an archival *XMM-Newton* observation that included G311.5−0.3 in the field of view: this is the first time that *XMM-Newton* data has been used to probe the X-ray properties of this SNR. The *XMM-Newton* observation confirms that the X-ray emission from G311.5−0.3 is centrally concentrated and supports the classification of this source as a mixed-morphology SNR. In addition, our joint fitting of extracted *ASCA* and *XMM-Newton* spectra favor a thermal origin for the X-ray emission over a non-thermal origin. The spectral fitting parameters for our TBABS×APEC fit to the extracted spectra are $N_{\rm H}$ = $4.63^{+1.87}_{-0.85}\times10^{22}$ cm^{-2} and kT = $0.68^{+0.20}_{-0.24}$ keV. From these fit parameters, we derive the following values for physical parameters of the SNR: $n_{\rm e}$ = 0.20 cm^{-3}, $n_{\rm p}$ = 0.17 cm^{-3}, $M_{\rm X}$ = 21.4 $M_{\odot}$ and P/k = 3.18×10^{6} K cm^{-3}.

Key words. ISM: individual objects: G311.5−0.3 – ISM: supernova remnants – X-rays: individuals: G311.5−0.3 – X-rays: ISM

1. INTRODUCTION

Supernova remnants (SNRs) originate from the violent deaths of stars (either massive stars or degenerate stars in binary systems) in supernova (SN) explosions. Studies of SNRs yield insights into a variety of associated physical phenomena such as the endpoints of stellar evolution, the chemical and tem-

poral evolution of the interstellar medium (ISM) in galaxies and the acceleration of cosmic-ray particles. SNRs manifest themselves across the entire electromagnetic spectrum through a variety of emission mechanisms and therefore observations made at multiple wavelength domains are often considered simultaneously in the study of particular SNRs of interest. Nearly 300 Galactic SNRs are known to exist (Green 2014, 2017) but only a small minority of these sources have been the subjects of extensive study at multiple wavelength domains. Such studies are absolutely vital for developing a coherent understanding of SNRs and related physical phenomena.

In this paper we present an analysis of X-ray observations made of the Galactic SNR G311.5−0.3 with the Advanced Satellite for Cosmology and Astrophysics (*ASCA*) and *XMM-Newton*. This source was first detected by radio observations, which revealed a shell-like morphology for the SNR with an angular diameter of approximately 5′, an integrated flux density ∼3 Jy at 1 GHz and a spectral index $\alpha \sim -0.5$[1] (Shaver and Goss 1970, Caswell and Barnes 1985, Whiteoak and Green 1996). Recent infrared imaging and spectroscopic observations made with the *Spitzer* Space Telescope have yielded dramatic new insights into the properties of G311.5−0.3. Imaging observations made with *Spitzer* reveal a shell-like morphology for the SNR at all four IRAC channels (Reach et al. 2006) and at both MIPS channels (Pinheiro Gonçalves et al. 2011). Reach et al. (2006) also measured IRAC colors for G311.5−0.3 at the four IRAC channels and argued that the IRAC-detected emission from the SNR was produced by shocked molecules, suggesting that G311.5−0.3 is interacting with adjacent molecular clouds. Complementary spectroscopic observations with the IRS clearly detected both H_2 lines (again suggesting interaction with adjacent molecular clouds) and ionic lines (such as [Ne II] and [Ne III]): the latter set of lines suggested the presence of a rather fast shock with a velocity 40-90 km s^{-1} propagating into a medium with an initial density of 10^4 cm^{-3} (Andersen et al. 2011).[2]

The scenario where G311.5−0.3 is interacting with adjacent molecular clouds gained additional support from Pannuti et al. (2014a) who analyzed CO observations made along the line of sight to this SNR and argued for a physical association between G311.5−0.3 and a molecular cloud with a radial velocity $v_{\rm LSR}$ = 39.7 km s^{-1}. Andersen et al. (2011) estimated a distance to the SNR of 14.8 kpc based on the radial velocity of the associated molecular cloud: we adopt this distance to G311.5−0.3 for the remainder of this paper.[3]We also note that G311.5−0.3 has been detected in the γ-ray: in their catalog of SNRs detected by *Fermi*, Acero et al. (2016) measure a flux of $16.54\pm1.16^{+11.60}_{-6.82} \times 10^{-9}$ photons cm^{-2} s^{-1} from G311.5−0.3 and a fitted photon index of $\Gamma = 2.51\pm0.09\pm0.10$ to the detected emission over the energy range of 1 to 100 GeV. While the nature of this detected γ-ray emission from G311.5−0.3 has yet to be explored, such high energy emission associated with SNRs is sometimes interpreted as originating from an interaction between the SNR and an adjacent molecular cloud. For example, γ-ray emission has been detected at the site of interaction between the Galactic SNR G347.3−0.5 (RX J1713.7−3946) (Acero et al. 2017) and adjacent molecular clouds and the origin of this high energy emission has been attributed to the decay of pions produced by collisions of cosmic-ray protons accelerated by the SNR with hydrogen nuclei in these molecular clouds (Fukui et al. 2003, Moriguchi et al. 2005), although this scenario is still debated in the literature (Acero et al. 2015).

The X-ray properties of G311.5−0.3 remain poorly explored in the literature: this is due in part to the large estimated distance to the SNR and the corresponding extensive Galactic absorption along the line of sight. The X-ray emission from G311.5−0.3 was detected for the first time by Pannuti et al. (2014a) who conducted an imaging and spectroscopic analysis of an archival pointed *ASCA* observation made of the SNR. Those authors extracted GIS2 and GIS3 images and spectra for the SNR: the combined GIS2+GIS3 image revealed a centrally-concentrated X-ray morphology rather than a shell-like morphology typically seen for Galactic SNRs. The two extracted spectra were fit simultaneously using a power law model and a thermal model known as APEC (Astrophysical Plasma Emission Code), which is an optically-thin collisionally-ionized plasma with solar abundances (Foster et al. 2012). Statistically acceptable fits to the spectra were obtained using either model (χ^2_ν=0.79 and 0.57, respectively) and the derived column densities for the two fits were comparable ($N_{\rm H}\sim3\times10^{22}$ cm^2). While the derived temperature for the APEC fit ($kT=0.98^{+1.02}_{-0.22}$ keV) is broadly consistent with the fitted temperatures of the X-ray emitting plasmas associated with other SNRs, the derived photon index for the power law fit ($\Gamma=4.82^{+3.78}_{-2.32}$) is more difficult to interpret physically, since it appears to fall between values expected for synchrotron emission and for thermal bremsstrahlung emission, the emission mechanisms typically detected by X-ray observations of Galactic SNRs (Vink 2012).

[1]We adopt here the convention that α is defined as $S_\nu \propto \nu^\alpha$.

[2]In fact, generally, in the case of G311.5−0.3, the ionic lines suggest a moderately fast shock, while specifically the [Ne III]-to-[Ne II] ratio points towards either a shock of 100 km s^{-1} or a faster shock of approximately 170 km s^{-1} with different number densities.

[3]This distance estimate is consistent with distance estimates to G311.5−0.3 that have employed other methods. For example, Pavlović et al. 2014 derived a distance estimate to G311.5−0.3 of 12.8 kpc using the radio surface brightness to diameter relation (also known as the Σ-D relation) for Galactic SNRs.

Uncertainty in the true X-ray properties of G311.5−0.3 motivates the present work, where we conduct a spatial and spectroscopic analysis of archival *ASCA* and *XMM-Newton* observations of the SNR. The main goal of the present work is to build on the previous X-ray study conducted of G311.5−0.3 by Pannuti et al. (2014a) and improve our understanding of both the X-ray morphology and the X-ray emission mechanism of this SNR. The organization of this paper may be described as follows: the observations and the accompanying data reduction procedures are presented in Section 2, specifically the *ASCA* and *XMM-Newton* observations in Sections 2.1 and 2.2, respectively. The results are presented in Section 3 where we discuss the results of our imaging and spectroscopic analysis in Sections 3.1 and 3.2, respectively. Lastly, the results of this paper are given in Section 4.

2. OBSERVATIONS AND DATA REDUCTION

Below we describe the *ASCA* and *XMM-Newton* observations of G311.5−0.3 and the accompanying data reduction processes. Details about the observations are summarized in Tables 1 and 2 and the data reduction steps were performed using standard tools (namely FTOOLS[4]) in the HEASOFT software package Version 6.19.

2.1. *ASCA* observations and data reduction

G311.5−0.3 was the subject of a pointed observation made by *ASCA* on 2$^{\rm nd}$ March 1996 (OBSID 56047000, PI: John Hughes) with the SIS0, SIS1, GIS2 and the GIS3. The signal-to-noise levels of the data collected by the former two instruments were too low for a detailed analysis and they are not considered in the present paper. During this observation, G311.5−0.3 was located $\sim 7\farcm9$ off-axis.

The dataset was downloaded from the archive located at the High Energy Astrophysics Science Archive Research Center (HEASARC[5]). The data were reduced in an identical manner to the steps taken by Pannuti et al. (2014a) where `xselect` applied standard screening to the GIS datasets: after applying this screening, the effective exposure times of the observations were 17858 seconds and 17870 seconds, respectively. GIS2 and GIS3 source spectra were extracted from a circular source region centered on the coordinates RA(J2000.0)=$14^{\rm h}05^{\rm m}35\fs03$, Dec(J2000.0)=$-61°58'18\farcs2$ and with a radius of $150''$. Background spectra were extracted from an annular region extending $60''$ beyond the source region: in this way, the data reduction differed from the reduction performed by Pannuti et al. (2014a) where the FTOOL `mkgisbgd` was used to generate spectra for background subtraction. A different approach was taken here in extracting a background spectrum to be consistent with the spectral analysis of the *XMM-Newton* observation of G311.5−0.3 (see Section 2.2). Specifically, in the analysis of the *XMM-Newton* data, background spectra were extracted from this annular region and we thus took the same approach when choosing the method for extraction of background spectra. For spectral fitting, canned redistribution matrix files (RMFs) were used and the FTOOL `ascaarf` was implemented to create ancillary response files (ARFs), The GIS2 and GIS3 source spectra were both grouped to a minimum of 25 counts per bin using the FTOOL `grppha`. Lastly, we used the FTOOL `addaspec` to merge the two source spectra (along with the background spectra and the ARFs).

Table 1. Summary of *ASCA* GIS2+GIS3 Observations of G311.5−0.3.

Sequence Number	Right Ascension (J2000.0)	Decl. (J2000.0)	GIS2 Effective Exp. Time (s)	GIS2 Count Rate[a] (counts s^{-1})	GIS3 Effective Exp. Time (s)	GIS3 Count Rate[a] (counts s^{-1})
56047000	14 06 18.7	−61 53 02	17858	4.2×10^{-3}	17870	6.2×10^{-3}

Table 2. Summary of *XMM-Newton* MOS1+MOS2+PN Observations of G311.5−0.3.

Sequence Number	Right Ascension (J2000.0)	Decl. (J2000.0)	MOS1 Effective Exposure Time (s)	MOS1 Count Rate[a] (counts s^{-1})	MOS2 Effective Exposure Time (s)	MOS2 Count Rate[a] (counts s^{-1})	PN Effective Exposure Time (s)	PN Count Rate[a] (counts s^{-1})
0007421601	14 05 13.5	−62 03 39	11970	7.1×10^{-3}	6553	8.8×10^{-3}	3961	1.3×10^{-2}

[4]http://heasarc.gsfc.nasa.gov/docs/software/ftools/ftools_menu.html.

[5]HEASARC is a service of the Laboratory for High Energy Astrophysics at the National Aeronautics and Space Administration Goddard Space Flight Center (NASA/GSFC) and High Energy Astrophysics Division of the Smithsonian Astrophysical Observatory. For more information on HEASARC, please see http://heasarc.gsfc.nasa.gov.

2.2. *XMM-NEWTON* observations and data reduction

G311.5−0.3 was serendipitously observed by *XMM-Newton* on 20$^{\rm th}$ February 2002 (OBSID 0007421601, PI: Arvind Parmar) with the MOS1, MOS2 and the PN cameras in Medium Filter Imaging mode. During this observation, G311.5−0.3 was located $\sim 7\farcm4$ off-axis.

The dataset for the observation was downloaded from the on-line *XMM-Newton* data archive[6] and processed in a similar manner to the processing of *XMM-Newton* datasets as described in our previous works (Pannuti et al. 2014a,b) of observations of other Galactic SNRs. In summary, the dataset was processed with Science Analysis Software (SAS) Package Version 15.0.0 (Gabriel et al. 2004): the SAS tools `emchain` and `mos − filter` were used to apply standard data reduction steps and perform background flare filtering, respectively, on the MOS1 and MOS2 observations while the SAS tools `epchain` and `pn − filter` were used to apply standard data reduction steps and perform background flare filtering on the PN observation.

After processing, the effective exposure times of the MOS1, MOS2 and PN observations were 11970, 6553 and 3961 seconds, respectively. Source spectra of G311.5−0.3 for all three cameras (along with accompanying background spectra) were extracted using the SAS tool `evselect` and with the same extraction regions that were used for generating the *ASCA* GIS spectra.

In parallel to our analysis of the *ASCA* GIS spectra, the extracted source spectra were grouped to a minimum of 25 counts per bin. The SAS tool `backscale` was then used to determine the proper value for the BACKSCAL keyword in each of the extracted MOS1, MOS2 and PN spectra. Next, the SAS tools `arfgen` and `rmfgen` were used to create the ARFs and RMFs respectively for each source spectrum. Finally, to improve the statistics of the spectral analysis, the SAS tool `epicspeccombine` was run to merge all three of the source spectra as well as merge all three of the background spectra and generate an appropriate response matrix file for the merged source spectrum.

3. RESULTS

3.1. Imaging

In Fig. 1 we present an exposure-corrected and co-added (MOS1+MOS2+PN) *XMM-Newton* image of G311.5−0.3. This image has also been smoothed with a Gaussian with a radius of $15''$. For illustrative purposes, we have also overlaid contours depicting the radio emission as detected at 843 MHz by the Molonglo Observatory Synthesis Telescope (MOST): this radio observation of G311.5−0.3 has been described and analyzed in detail by Whiteoak and Green (1996).

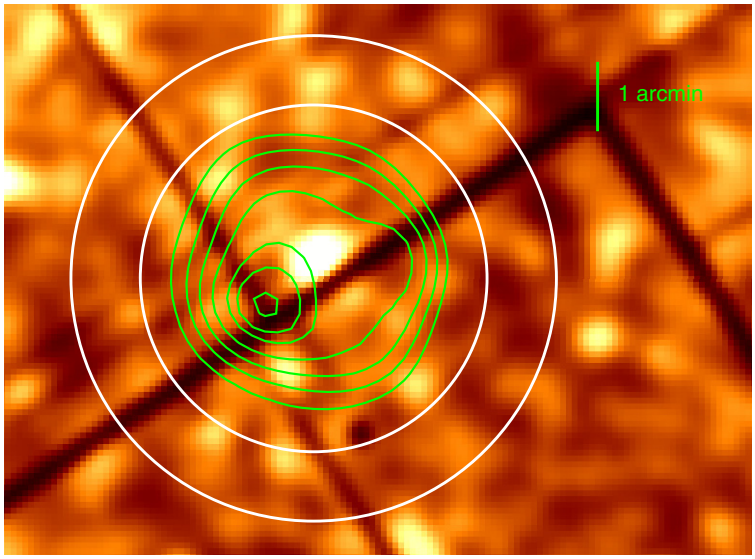

Fig. 1. *Combined MOS1+MOS2+PN exposure-corrected image of G311.5−0.3 with contours overlaid depicting emission detected at 843 MHz by the Molonglo Observatory Synthesis Telescope (MOST) (see Whiteoak and Green 1996). The contour levels correspond to 0.08, 0.12, 0.16, 0.2, 0.24, 0.26 and 0.28 Jy/beam. The inner white circle indicates the region of spectral extraction for the source spectrum while the outer white circle indicates the surrounding annular region of spectral extraction for the background spectrum. The regions of spectral extraction are the same for the ASCA and XMM-Newton observations. The X-ray emission has been smoothed by a Gaussian with a radius of 15 arcseconds.*

[6] http://xmm.esac.esa.int/xsa/.

Consistent with our analysis of the *ASCA* GIS2+GIS3 images of this SNR presented in Pannuti et al. (2014a), the X-ray emission from G311.5−0.3 does not match the shell-like radio morphology of the SNR but is instead centrally concentrated. This contrast in morphologies – coupled with the likely thermal origin of the X-ray emission as discussed in Section 3.2 – motivates the classification of G311.5−0.3 as a mixed-morphology SNR. These SNRs are characterized by this combination of contrasting morphologies in the X-ray and radio (Rho and Petre 1998, Chen et al. 2008): well-known examples of Galactic mixed-morphology SNRs include W28 (Rho and Borkowski 2002, Pannuti et al. 2017), W44 (Shelton et al. 2004, Uchida et al. 2012), G332.5-5.6 (Stupar et al. 2007) and W49B (Keohane et al. 2007, Lopez et al. 2013).

While the origin of the contrasting morphologies for these particular sources remains unclear, it is noted that as a general trend, mixed-morphology SNRs all appear to be interacting with adjacent molecular clouds (Vink 2012) and therefore this interaction is believed to play a role in fostering the center-filled thermal X-ray emission seen from these sources. In addition to its center-filled X-ray morphology, G311.5−0.3 appears to resemble other mixed-morphology SNRs in other ways, namely in its interaction with an adjacent molecular cloud as evidenced by its infrared morphology and spectral properties as described in Section 1.

Unfortunately, the low signal-to-noise of the merged image of G311.5−0.3 does not provide a very clear contrast between the X-ray emission from the center of the SNR and its outer rim: furthermore, the presence of a prominent pulsar wind nebula (PWN) in the center of this SNR cannot be completely ruled out with the present datasets. Additional deep X-ray observations with improved sensitivity are necessary to investigate the true X-ray morphology of G311.5−0.3 and to determine if a PWN is seen in the interior of this SNR.

3.2. Spectroscopy

The spectral fitting was performed using the XSPEC software package Version 12.9.0n (Arnaud 1996). The extracted spectra were fit over the energy range of 1.0 keV to 4.0 keV with the same power law and APEC models that were considered by Pannuti et al. (2014a): once again, the elemental abundances of the latter model were fixed to solar. In contrast to our previous work, we convolve these two models with the Tübingen-Boulder interstellar absorption model TBABS: also, the interstellar elemental abundances developed by Wilms et al. (2000) were adopted. This particular absorption model – instead of other absorption models, like WABS and PHABS (the latter was implemented in the previous work that we presented in Pannuti et al. (2014a)) – was chosen to use the most up-to-date measurements of interstellar elemental abundances. We also note that the low overall signal-to-noise of the datasets motivates the use of only simpler models in the spectral analysis, such as a power law and APEC (this latter model assumes that the X-ray-emitting plasma is in collisional ionization equilibrium). The present datasets lack enough signal to apply more sophisticated models that have been applied to fitting extracted X-ray spectra of other MMSNRs. These models include VNEI (a non-equilibrium ionization collisional plasma model with variable elemental abundances) and VRNEI (a non-equilibrium ionization recombining plasma model with variable elemental abundances). The reader is referred to Borkowski et al. (2001) for more details about these non-equilibrium ionization models.

In Table 3, we present the results of our spectral fitting with these two models: consistent with the results of Pannuti et al. (2014a), we obtain statistically acceptable fits ($\Delta\chi^2 \sim 1.0$) to the extracted spectra using the power law and the APEC model. However, in contrast to that previous work – where

Table 3. Summary of Fits to *ASCA* GIS2+GIS3 and *XMM-Newton* MOS1+MOS2+PN Spectra of G311.5−0.3. Both models have been convolved with the interstellar absorption model TBABS. All quoted error bounds correspond to the 90% confidence level.

Model	$N_{\rm H}$ (10^{22} cm^{-2})	kT (keV)	Γ^b	K^c	χ^2_ν (χ^2/DOF)	Unabsorbed Flux^d (ergs cm^{-2} s^{-1})	Unabsorbed Luminosity^d (ergs s^{-1})
Power Law	$7.24^{+3.60}_{-2.74}$	–	6.90(>4.68)	2.53×10^{-2}	1.01 (662.49/657)	8.29×10^{-12}	2.17×10^{35}
APEC^e	$4.63^{+1.87}_{-0.85}$	$0.68^{+0.20}_{-0.24}$	–	3.07×10^{-3}	0.99 (647.25/657)	1.56×10^{-12}	4.09×10^{34}

^{b}Defined such that the dependence of flux on energy E is proportional to $E^{-\Gamma}$.
^{c}K is the normalization value. In the case of the Power Law model, K is defined in units of photons keV^{-1} cm^{-2} s^{-1} at 1 keV. In the case of the APEC model, K is in units of (cm^{-5}) and defined as $(10^{-14}/4\pi d^2)\times\int n_{\rm e} n_{\rm p} dV$, where d is the distance to the source (in units of cm), $n_{\rm e}$ and $n_{\rm p}$ are the number densities of electrons and hydrogen nuclei, respectively (in units of cm^{-3}) and finally $\int dV = V$ is the integral over the entire volume of the X-ray-emitting plasma (in units of cm^{-3}).
^{d}Measured over the energy range of 1.0 to 4.0 keV. The luminosities are computed assuming a distance to G311.5−0.3 of 14.8 kpc.
^{e}Abundance parameter frozen to solar values.

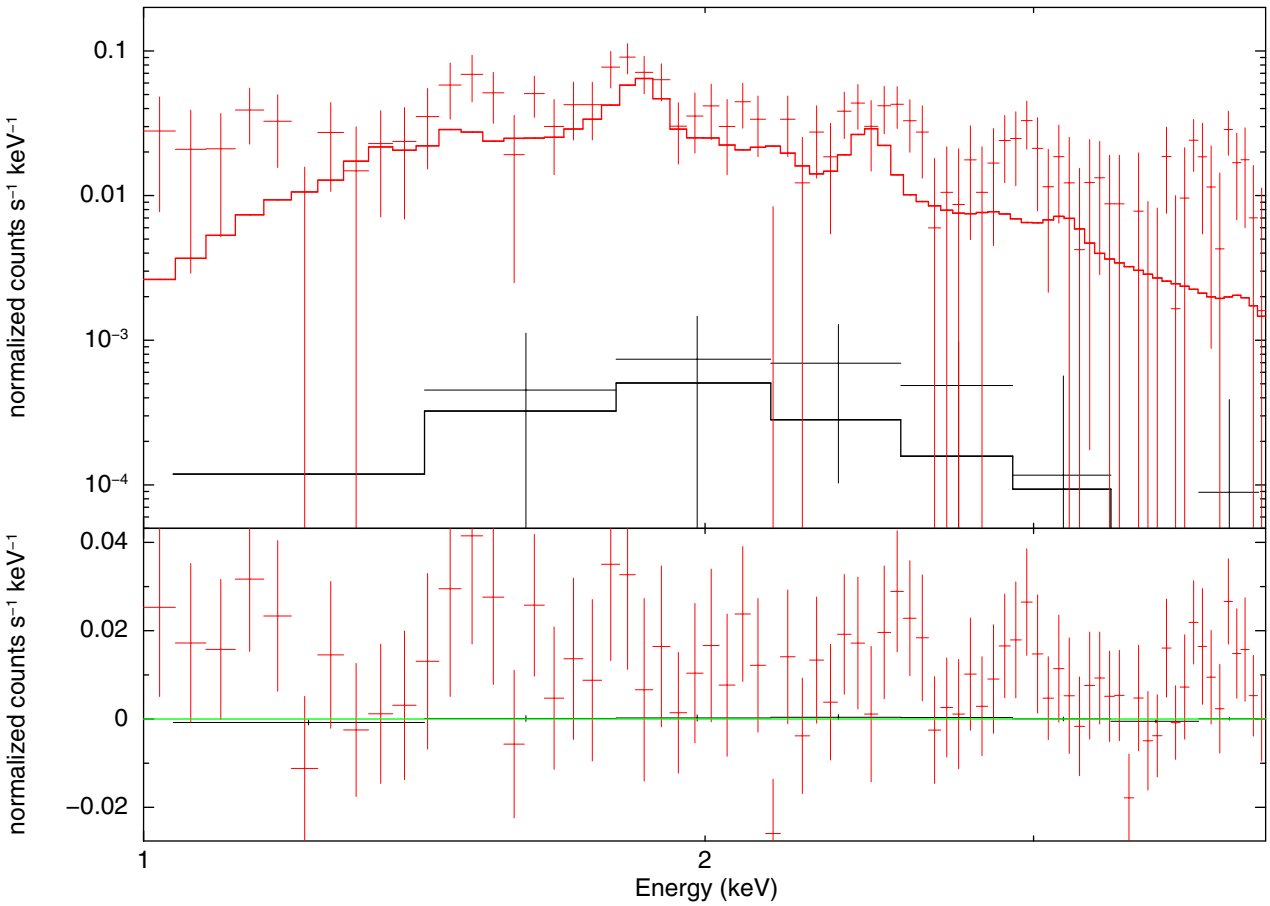

Fig. 2. *(Top Panel) The combined ASCA GIS2+GIS3 spectra and XMM-Newton MOS1+MOS2+PN spectra (shown in black and red respectively) of G311.5−0.3. The source and background spectra have been extracted from the extraction regions shown in Fig. 1 and the spectra are fitted with the parameters of the TBABS×APEC fit listed in Table 3. (Bottom Panel) The residuals of the fits to the extracted spectra by the TBABS×APEC model.*

the large errors in the values of the fit parameters prevented a clear classification of the X-ray emission process associated with the plasma as either synchrotron or thermal bremsstrahlung – it is possible to interpret the fit parameters much more clearly and address this question. The very steep value of the photon index of the TBABS×Power Law fit (Γ=6.82(>4.67)) are consistent with values expected for fitting a thermal bremsstrahlung spectrum.

Furthermore, for the TBABS×APEC fit, the fitted temperature value (kT=$0.68^{+0.20}_{-0.24}$ keV) is both broadly consistent with the fitted value derived by Pannuti et al. (2014a) and more consistent with the fitted temperatures derived for the X-ray emitting plasmas associated with other SNRs. In Fig. 2 we present the merged *ASCA* GIS2+GIS3 and *XMM-Newton* MOS1+MOS2+PN spectra as fit by the parameters of the TBABS×APEC fit that is presented in Table 3. We therefore argue that the ambiguity about the nature of the X-ray emission from G311.5−0.3 is resolved: the emission is produced by a thermal plasma and not by synchrotron X-ray emission from the SNR nor by a PWN.

4. DISCUSSION

We now discuss the results of our analysis for G311.5−0.3 in the context of other MMSNRs. The fitted temperature of the X-ray emission from G311.5−0.3 (kT=$0.68^{+0.20}_{-0.24}$ keV) is comparable to the fitted temperatures derived in the analysis of the X-ray spectra of other MMSNRs. The flat radio spectral index of G311.5−0.3 is also consistent with the flat radio spectral indices measured for other MMSNRs. In addition, like other MMSNRs, there is robust evidence that G311.5−0.3 is interacting strongly with adjacent molecular clouds as revealed by its infrared colors and its infrared spectra. Finally, the X-ray emitting plasma of G311.5−0.3 may also be a recombining plasma dominated by over-

ionzation as seen in the spectra of other MMSNRs. However, at present, the available X-ray data for G311.5-0.3 lacks the signal-to-noise needed to confirm the presence of such plasma conditions associated with this SNR (if present). Additional X-ray observations of this SNR (such as an additional observation made with *XMM-Newton* with a much longer exposure time or a new observation made with the *Chandra* X-ray Observatory) are needed to probe the X-ray properties of G311.5−0.3 in more detail.

We now compute several salient properties of G311.5−0.3 based on the fitted parameters to the extracted X-ray spectra using the TBABS×APEC model. These are the same properties of the SNR that were examined and quantified previously by Pannuti et al. (2014a): here, we refine these computations based on the new fit parameters to the extracted spectra of G311.5−0.3 and the new adopted distance to the SNR (note that Pannuti et al. 2014a had previously assumed a lower distance to G311.5−0.3 of 12.5 kpc).

The electron number density $n_{\rm e}$ (and, in turn, the X-ray emitting mass $M_{\rm X}$) may be determined from the normalization K of the TBABS×APEC fit to the extracted spectra, which is defined as

$$K\,({\rm cm}^{-5}) = \frac{10^{-14}}{4\pi d^2} \int n_{\rm e} n_{\rm p} dV. \qquad (1)$$

Here, d is the distance to G311.5−0.3 in cm, $n_{\rm p}$ is the proton number density in cm^{-3} and $\int dV = V$ in cm^3 is the volume occupied by the X-ray emitting plasma. We assume that $n_{\rm e} = 1.2\ n_{\rm p}$ and that both number densities are uniform throughout the volume of the plasma: we further assume that the volume filling factor of the plasma is unity. Therefore, from this equation and the fitted normalization value of 3.07×10^{-3} cm^{-5}, we compute an electron number density $n_{\rm e} = 0.20$ cm^{-3} and a proton number density $n_{\rm p} = 0.17$ cm^{-3}. At the adopted distance to G311.5−0.3 and assuming a spherical geometry for the source, its volume is V=1.54×10^{59} cm^3 and thus $M_{\rm X} = n_{\rm p} m_{\rm p} V = 21.4\ M_\odot$ (where $m_{\rm p}$ is the mass of a proton). While the values of $n_{\rm e}$ and $n_{\rm p}$ are essentially identical to the values for these quantities that were computed by Pannuti et al. (2014a), the value of $M_{\rm X}$ is larger due to the greater assumed distance to the SNR.

Finally, we consider the pressure P expressed in units of cm^{-3} K as $P/k = 2 n_{\rm e} T$ where k is Boltzmann's constant. From the computed value of $n_{\rm e}$ and the fitted value for T in the TBABS×APEC model, we compute $P/k = 2$ (0.20 cm^{-3})(7.94×10^6 K) = 3.18×10^6 cm^{-3} K.

5. CONCLUSIONS

The conclusions of this paper may be summarized as follows:

- We have conducted a new joint *ASCA* and *XMM-Newton* spectral and spatial analysis of the X-ray emission from the Galactic SNR G311.5−0.3. Our work represents the first effort to analyze *XMM-Newton* data for this source through the use of an archival observation that serendipitously observed the source.
- We fit merged *ASCA* GIS2+GIS3 and *XMM-Newton* MOS1+MOS2+PN spectra of the SNR with first a simple power law model and then with a thermal (APEC) model: in both cases, the multiplicative absorption model TBABS was applied. While we find that both fits provide statistically acceptable fits, the extremely steep value for the photon index of the power law fit (specifically Γ=6.82>4.67) strongly favors a thermal origin for the X-ray emission over a different origin (from synchrotron X-ray emission or a central PWN). Our work therefore resolves that the observed X-ray emission from G311.5−0.3 is thermal in origin with a fitted temperature $kT = 0.68^{+0.20}_{-0.24}$ keV.
- Based on the parameters of the fit with a thermal model to the extracted spectra of G311.5−0.3, we have recomputed several salient physical properties of the SNR. These properties are $n_{\rm e} = 0.20$ cm^{-3}, $n_{\rm p} = 0.17$ cm^{-3}, $M_{\rm X} = 21.4\ M_\odot$ and $P/k = 3.18 \times 10^6$ cm^{-3} K.

These values are all broadly consistent with values for these properties that were previously computed by Pannuti et al. (2014a): minor differences may be attributed to the slightly larger distance assumed to this SNR than the previous work.

Acknowledgements – We thank the referee for multiple comments that have improved the quality of this paper. T.G.P. thanks Kip Kuntz and Steven Snowden for helpful discussions about the reduction and analysis of $XMM-Newton$ data. This research has made use of NASA's Astrophysics Data System as well as data, software and/or web tools obtained from the High Energy Astrophysics Science Archive Research Center (HEASARC), a service of the Astrophysics Science Division at NASA/GSFC and of the Smithsonian Astrophysical Observatory's High Energy Astrophysics Division.

REFERENCES

Acero, F., Lemoine-Goumard, M., Renaud, M. et al.: 2015, *Astron. Astrophys*, **580**, A74.
Acero, F., Ackermann, M., Ajello, M. et al.: 2016, *Astrophys. J. Suppl. Ser.*, **224**, 8.
Acero, F., Aloisio, R., Amans, J. et al.: 2017, *Astrophys. J.*, **840**, 74.
Andersen, M., Rho, J., Reach, W. T., Hewitt, J. W. and Bernard, J. P.: 2011, *Astrophys. J.*, **742**, 7.
Arnaud, K. A.: 1996, Astronomical Data Analysis Software and Systems V, **101**, 17.
Borkowski, K. J., Lyerly, W. J. and Reynolds, S. P.: 2001, *Astrophys. J.*, **548**, 820.

Caswell, J. L. and Barnes, P. J.: 1985, *Mon. Not. R. Astron. Soc.*, **216**, 753.
Chen, Y., Seward, F. D., Sun, M. and Li, J.-t.: 2008, *Astrophys. J.*, **676**, 1040.
Foster, A. R., Ji, L., Smith, R. K. and Brickhouse, N. S.: 2012, *Astrophys. J.*, **756**, 128.
Fukui, Y., Moriguchi, Y., Tamura, K. et al.: 2003, *Publ. Astron. Soc. Jpn.*, **55**, L61.
Gabriel, C., Denby, M., Fyfe, D. J. et al.: 2004, Astronomical Data Analysis Software and Systems (ADASS) XIII, **314**, 759.
Green, D. A.: 2014, *Bull. Astr. Soc. India*, **42**, 47.
Green D. A.: 2017, A Catalogue of Galactic Supernova Remnants (2017 June version), Cavendish Laboratory, Cambridge, United Kingdom (available at *http://www.mrao.cam.ac.uk/surveys/snrs/*).
Keohane, J. W., Reach, W. T., Rho, J. and Jarrett, T. H.: 2007, *Astrophys. J.*, **654**, 938.
Lopez, L. A., Pearson, S., Ramirez-Ruiz, E. et al.: 2013, *Astrophys. J.*, **777**, 145.
Moriguchi, Y., Tamura, K., Tawara, Y. et al.: 2005, *Astrophys. J.*, **631**, 947.
Pannuti, T. G., Rho, J., Heinke, C. O. and Moffitt, W. P.: 2014a, *Astron. J*, **147**, 55.
Pannuti, T. G., Kargaltsev, O., Napier, J. P. and Brehm, D.: 2014b, *Astrophys. J.*, **782**, 102.
Pannuti, T. G., Rho, J., Kargaltsev, O. et al.: 2017, *Astrophys. J.*, **839**, 59.
Pavlović, M. Z., Dobardžić, A., Vukotić, B. and Urošević, D.: 2014, *Serb. Astron. J.*, **189**, 25.
Pinheiro Gonçalves, D., Noriega-Crespo, A., Paladini, R., Martin, P. G. and Carey, S. J.: 2011, *Astron. J*, **142**, 47.
Reach, W. T., Rho, J., Tappe, A. et al.: 2006, *Astron. J*, **131**, 1479.
Rho, J. and Petre, R.: 1998, *Astrophys. J.*, **503**, L167.
Rho, J. and Borkowski, K. J.: 2002, *Astrophys. J.*, **575**, 201.
Shaver, P. A. and Goss, W. M.: 1970, *Australian Journal of Physics, Astrophysical Supplement*, **14**, 133.
Shelton, R. L., Kuntz, K. D. and Petre, R.: 2004, *Astrophys. J.*, **611**, 906.
Snowden, S. L. and Kuntz, K. D.: 2011, *Bulletin of the American Astronomical Society*, **43**, 344.17.
Stupar, M., Parker, Q. A., Filipović, M. D., Frew, D. J., Bojičić, I. and Aschenbach, B.: 2007, *Mon. Not. R. Astron. Soc.*, **381**, 377.
Uchida, H., Koyama, K., Yamaguchi, H. et al.: 2012, *Publ. Astron. Soc. Jpn.*, **64**, 141.
Vink, J.: 2012, *Astron. Astrophys. Rev.*, **20**, 49.
Whiteoak, J. B. Z. and Green, A. J.: 1996, *Astron. Astrophys*, **118**, 329.
Wilms, J., Allen, A. and McCray, R.: 2000, *Astrophys. J.*, **542**, 914.

ASCA И XMM-NEWTON ПОСМАТРАЊА ГАЛАКТИЧКОГ ОСТАТКА СУПЕРНОВЕ G311.5−0.3

T. G. Pannuti[1], M. D. Filipović[2], K. Luken[2], G. F. Wong[2,3], P. Manojlović[2], N. Maxted[3,2] and Q. Roper[2]

[1] *Department of Earth and Space Sciences, Morehead State University*
235 Martindale Drive, Morehead, KY 40351, USA

E–mail: *t.pannuti@moreheadstate.edu*

[2] *Western Sydney University, Locked Bag 1797, Penrith NSW 2751, Australia*

E–mail: *m.filipovic@westernsydney.edu.au*

[3] *School of Physics, The University of New South Wales, Sydney, 2052, Australia*

УДК 524.354–795
Оригинални научни рад

У овој студији представљамо анализу рендгенских посматрања (ASCA и XMM-NEWTON) галактичког остатка супернове – G311.5−0.3. Претходна инфрацрвена и радио-посматрања овог остатка указују на љускасту морфологију. Радио-спектрални индекс остатка је конзистентан са синхротронским зрачењем а инфрацрвена посматрања са емисијом молекуларног водоника поремећеног ударним таласом. Такође претходна CO посматрања указују на интеракцију између самог остатка и молекуларног облака који се налази у близини G311.5−0.3. Наша претходна анализа ASCA рендгенских посматрања је потврдила постојање овог остатка али је лошија резолуција спречила дубљу анализу. Анализирали смо и старија (архивирана) рендгенска посматрања са телескопа XMM-NEWTON. Ова посматрања су потврдила да је рендгенска емисија концентрисана ка центру овог остака што је различито од радио-емисије која је љускастог типа. Ове различите емисије указују да G311.5−0.3 припада групи тзв. мешане морфологије остатака супернових. Наша нова фитовања ASCA и XMM-NEWTON спектра фаворизују термалну емисију рендгенског зрачења. Спектрални параметри фита за наш TBABS×APEC екстрактовани спектар су $N_{\rm H} = 4.63^{+1.87}_{-0.85}\times10^{22}$ cm^{-2} и $kT = 0.68^{+0.20}_{-0.24}$ keV. Из ових параметара фита добили смо следеће вредности за овај остатак: $n_{\rm e} = 0.20$ cm^{-3}, $n_{\rm p} = 0.17$ cm^{-3}, $M_{\rm X} = 21.4\ M_{\odot}$ и $P/k = 3.18\times10^{6}$ K cm^{-3}.